DTNSRDC/SPD-0991-02

DAVID W. TAYLOR NAVAL SHIP RESEARCH AND DEVELOPMENT CENTER

Bethesda, Maryland 20084

PREDICTION OF HYDRODYNAMIC PRESSURES ON THE BULBOUS BOW OF A SHIP MOVING IN WAVES

by

Choung M. Lee

and

William C. Meyers

DISTRIBUTION UNLIMITED: APPROVED FOR PUBLIC RELEASE

SHIP PERFORMANCE DEPARTMENT
DEPARTMENTAL REPORT

JUNE 1981

DTNSRDC/SPD-0991-02

PREDICTION OF HYDRODYNAMIC PRESSURES ON THE BULBOUS BOW
OF A SHIP MOVING IN WAVES by Choung M. Lee and William C. Meyers

MAJOR DTNSRDC ORGANIZATIONAL COMPONENTS

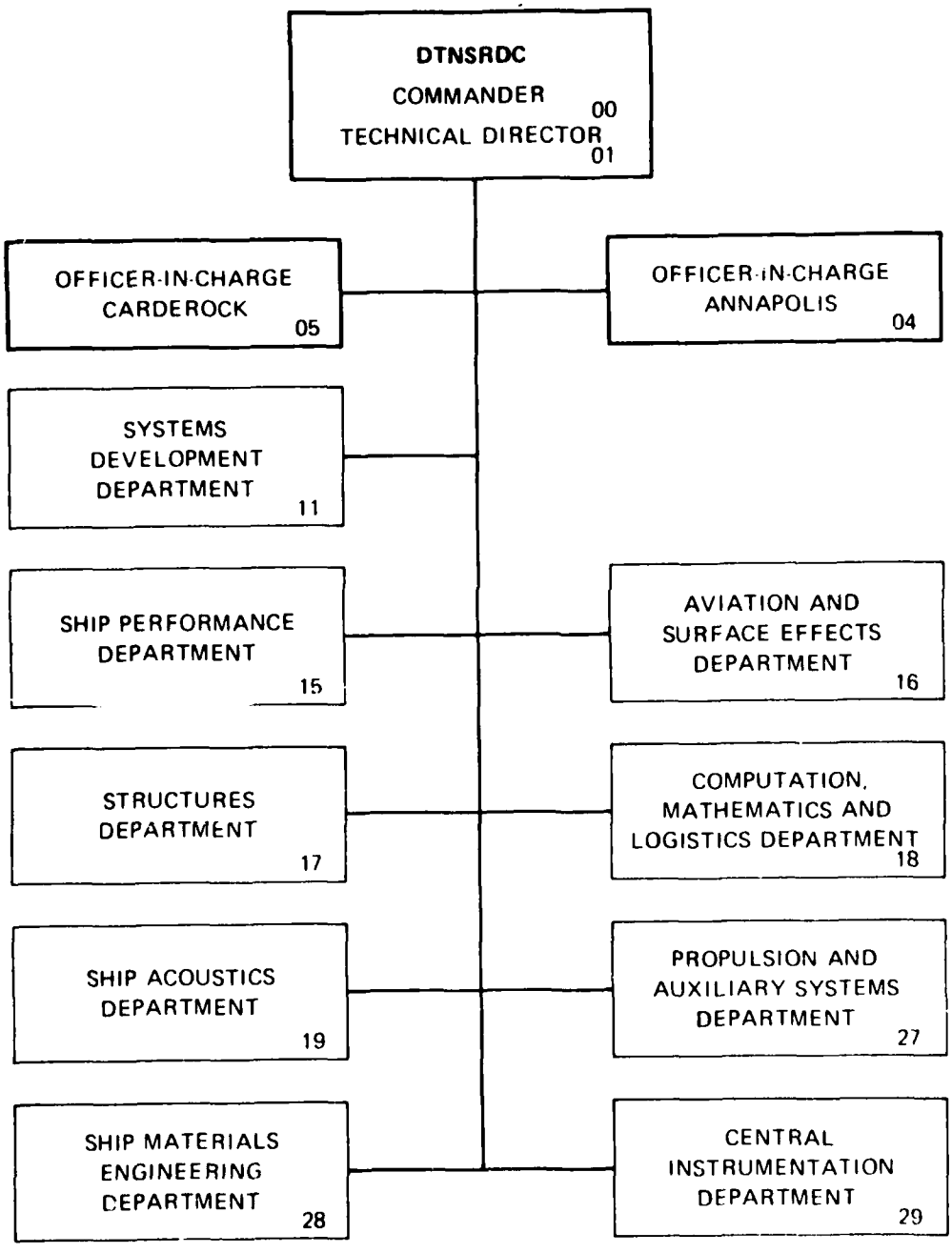

UNCLASSIFIED

SECURITY CLASSIFICATION OF THIS PAGE *(When Data Entered)*

REPORT DOCUMENTATION PAGE		READ INSTRUCTIONS BEFORE COMPLETING FORM
1. REPORT NUMBER DTNSRDC/SPD-0991-02	2. GOVT ACCESSION NO. AD-A100 067	3. RECIPIENT'S CATALOG NUMBER
4. TITLE *(and Subtitle)* PREDICTION OF HYDRODYNAMIC PRESSURES ON THE BULBOUS BOW OF A SHIP MOVING IN WAVES		5. TYPE OF REPORT & PERIOD COVERED Final Rept.
		6. PERFORMING ORG. REPORT NUMBER
7. AUTHOR(s) Choung M. Lee and William G. Meyers		8. CONTRACT OR GRANT NUMBER(s)
9. PERFORMING ORGANIZATION NAME AND ADDRESS David Taylor Naval Ship R&D Center Bethesda, Maryland 20084		10. PROGRAM ELEMENT, PROJECT, TASK AREA & WORK UNIT NUMBERS O&MN Project, Work Unit 1730-105
11. CONTROLLING OFFICE NAME AND ADDRESS Naval Sea Systems Command Washington, D.C.		12. REPORT DATE June 1981 13. NUMBER OF PAGES 32
14. MONITORING AGENCY NAME & ADDRESS*(If different from Controlling Office)*		15. SECURITY CLASS. *(of this report)* UNCLASSIFIED 15a. DECLASSIFICATION DOWNGRADING SCHEDULE

16. DISTRIBUTION STATEMENT *(of this Report)*

APPROVED FOR PUBLIC LELEASE: DISTRIBUTION UNLIMITED

17. DISTRIBUTION STATEMENT *(of the abstract entered in Block 20, if different from Report)*

18. SUPPLEMENTARY NOTES

19. KEY WORDS *(Continue on reverse side if necessary and identify by block number)*

Hydrodynamic Pressures; Ship Motion in Waves; Wave Induced Pressures; Strip Theory

20. ABSTRACT *(Continue on reverse side if necessary and identify by block number)*

Theoretical prediction of oscillatory pressures on the sonar dome of a CGN-38 Class ship proceeding in waves is made using a strip theory. The predicted values are compared with the measured values from a model experiment. Five locations on the dome are chosen for the comparison, and agreement between predicted and measured values is good except for the pressures at a point on the bottom side of the dome.

The good agreement is considered to be attributed to the fact that the

DD FORM 1 JAN 73 1473 EDITION OF 1 NOV 65 IS OBSOLETE

S/N 0102-LF-014-6601

UNCLASSIFIED

SECURITY CLASSIFICATION OF THIS PAGE *(When Data Entered)*

pressure head change due to the oscillatory vertical displacement of the dome, which is predicted reasonably well by the strip theory, is the dominant effect on the oscillatory pressures. The reason for the discrepancy between predicted and measured results on the bottom side of the dome may be due to shortcomings of the strip theory, but this question is unresolved.

TABLE OF CONTENTS

LIST OF TABLES

LIST OF FIGURES

NOTATION

g	Gravitational acceleration
K	Wave number; $K = \omega^2/g = 2\pi/\lambda$
L	Length between perpendiculars
$\overline{P}_i$	Nondimensional pressure amplitude at the ith gage (see Equation (7))
P_h, P_s, P_v, P_w	Definitions given in Equations (8); $(\overline{P}_h, \overline{P}_s, \overline{P}_v, \overline{P}_w) = (P_h, P_s, P_v, P_w)/(\rho g \zeta_A)$
U	Forward velocity of ship
(x,y,z)	Right-handed Cartesian coordinates (definition given below Equation (2))
α	Phase angle of pressure with respect to wave crest at the origin
β	Wave heading with respect to the positive x-axis; $\beta = \pi$ is head waves
ζ_A	Amplitude of incident wave
∇	Displaced volume of ship
λ	Length of incident wave
ξ_j	Complex amplitude of the displacement of ship in the jth mode of motion
ξ_v	Complex amplitude of vertical displacement of a point on the hull (see Equation (6))
ρ	Mass density of water
ϕ_j	Complex velocity potential associated with the jth mode of motion; $j = 7$ is the wave diffraction
Φ	Total velocity potential
ω	Wave frequency
ω_E	Wave-encounter frequency

ABSTRACT

Theoretical prediction of oscillatory pressures on the sonar dome of a CGN-38 Class ship proceeding in waves is made using a strip theory. The predicted values are compared with the measured values from a model experiment. Five locations on the dome are chosen for the comparison, and agreement between predicted and measured values is good except for the pressures at a point on the bottom side of the dome.

The good agreement is considered to be attributed to the fact that the pressure head change due to the oscillatory vertical displacement of the dome, which is predicted reasonably well by the strip theory, is the dominant effect on the oscillatory pressures. The reason for the discrepancy between predicted and measured results on the bottom side of the dome may be due to shortcomings of the strip theory, but this question is unresolved.

ADMINISTRATIVE INFORMATION

The work described in this report was performed as a part of continuing efforts at the David W. Taylor Naval Ship Research and Development Center (DTNSRDC) to develop operational guidelines for AN/SQS-26/53 Sonar Dome Rubber Windows. Funding was provided by Codes 63Y1 and 3213 of the Naval Sea Systems Command under O&MN Project, and is identified as DTNSRDC Work Unit 1730-105.

INTRODUCTION

A ship moving in waves is subjected to wave excited forces and moments, and as a result it undergoes oscillatory motion in an effort to maintain its equilibrium condition. In this process, the pressure acting at a point on the ship hull is contributed by several components. Under an assumption of small disturbance of fluid, these components can be identified as the incident wave, the diffracted wave, and the motions in six degrees of freedom. The motion-generated pressure can be decomposed into the components associated with the acceleration, velocity, and displacement (if the motion induces a vertical displacement of a point on the hull). The vertical displacement of a point on the hull from the rest position is directly related to the change in the pressure head $\rho g \Delta z$, where ρ is the water density, g the gravitational acceleration and Δz the vertical displacement.

Since the pressures on the hull constitute the basic source for obtaining the forces and moments on a ship's hull, it is appropriate to compare the computed pressures with the measured values as a meaningful verification of a theoretical

method. The present investigation is aimed at checking the validity of the strip theory for predicting the pressures on the hull of a ship moving in waves. Since pressure measurements taken on a sonar dome of a CGN-38 model are available,[1*] they are used to achieve the objectives of this investigation.

Despite initial concern that there would be a large discrepancy between the measured pressures and the predicted values, fairly good agreement was obtained. The concern was due to the realization that the flow around a sonar dome would hardly be two-dimensional, and the use of strip theory would be inappropriate. A close analysis of the pressure obtained by use of strip theory reveals that the unexpected good agreement is due to the fact that the major contribution to the pressures on the dome is the pressure-head change due to the vertical displacement of the dome, and that the strip theory predicts the vertical motion of the dome reasonably well.

The strip theory used in the present investigation is essentially that of Salvesen, et al.[2] except for a modification made to the wave-diffraction potential function such that it is independent of ship speed.

Comparison of the measured pressures with the computed values are presented in figures and tables, and are followed by pertinent discussions on the validity of the strip theory.

THEORETICAL PREDICTION OF PRESSURES

Under the assumption of an inviscid and irrotational motion of the fluid surrounding a ship, we can introduce the velocity potential function $\Phi(x,y,z,t)$ which represents the disturbance of the fluid at any field points. If the disturbance of the fluid is assumed to be small and harmonic in time, then one can linearly superimpose the various sources of the disturbances.

Thus, we can express the velocity potential by

$$\Phi = \mathrm{Re} \sum_{j=0}^{7} \xi_j \, \phi_j(x,y,z) \, e^{i\omega_E t} \qquad (1)$$

where Re means the real part of what follows; ξ_j the complex amplitude of the motion of the ship in the jth mode for $j = 1, 2, \ldots, 6$ and $\xi_0 = \xi_7 = 1$; ϕ_j the

*A complete listing of references is given on page 10.

complex velocity potential associated with the incident wave (j = 0), the jth mode of motion (j = 1 for surge, 2 for sway, 3 for heave, 4 for roll, 5 for pitch and 6 for yaw), and the diffracted wave (j = 7); $i = \sqrt{-1}$; and ω_E is the wave-encounter frequency which is related to the wave frequency ω, the wave headings β, and the ship speed U by

$$\omega_E = \omega - \frac{\omega^2}{g} U \cos \beta \tag{2}$$

The right-handed rectangular coordinate system 0-xyz is translating with the ship speed on the calm-water plane, and in the absence of incident waves, the origin is located directly above the center of gravity of the ship. The 0-x axis is directed toward the direction of the translation, the 0-y axis is directed to port, and the 0-z axis is directed vertically upward.

The complex amplitudes of the motion in six degrees of freedom can be obtained from the computation of ship motion in waves using Ship Motion Program (SMP)[3] developed at the Center.

The complex velocity potentials ϕ_j's, except ϕ_0, are obtained under the assumption of the two-dimensional flow condition at any transverse cross section of the ship. The details of the procedures for solving ϕ_j for j = 2, 3, . . ., 6 are described in References 2 and 5, and for ϕ_7 in Reference 6. No description for obtaining ϕ_1 will be given since the surge effect will be neglected in the pressure calculation later. The incident-wave potential ϕ_0 which represents progressive plane waves is given by

$$\phi_0 = \frac{ig\zeta_A}{\omega} e^{Kz - iK(x \cos \beta + y \sin \beta)} \tag{3}$$

where ζ_A is the amplitude, and $K = \omega^2/g$ is the wave number. From the slender-body strip theory,[2] we can show that

$$\phi_5(y,z;x) = -\left(x + \frac{U}{i\omega_E}\right) \phi_3(y,z;x) \tag{4a}$$

$$\phi_6(y,z;x) = \left(x + \frac{U}{i\omega_E}\right) \phi_2(y,z;x) \tag{4b}$$

If we let the pressure P(x,y,z,t) at any point on the hull to be expressed in the form

$$P = \mathrm{Re}[p(x,y,z)\ e^{i\omega_E t}]$$

we have from the Bernoulli equation

$$p = -\rho(i\omega_E - U\frac{\partial}{\partial x})\sum_{j=0}^{7}\xi_j\phi_j - \rho g(z+\xi_v) + O(\phi_j^2)$$

$$= -\rho[i\omega(\phi_0+\phi_7) + i\omega_E(\phi_1\xi_1+\phi_4\xi_4)$$

$$+ i\omega_E\phi_2\{\xi_2 + (x + \frac{i2U}{\omega_E})\xi_6\}$$

$$+ i\omega_E\phi_3\{\xi_3 - (x + \frac{i2U}{\omega_E})\xi_5\}]$$

$$- \rho g(z+\xi_3 - x\xi_5 + y\xi_4) + O(\phi_j^2) \qquad (5)$$

where ρ is the water density, and ξ_v is the complex amplitude of the vertical motion of the point on the hull which is given by

$$\xi_v = \xi_3 - x\xi_5 + y\xi_4 \qquad (6)$$

Note that the pressure contributed by the diffracted waves is given by $-i\rho\omega\phi_7(\omega)$ where one can observe that ϕ_7 is a function of ω rather than of ω_E. The rationale behind this is explained in Reference 4.

We can readily obtain the amplitude of the pressure by taking the absolute value of Equation (5) and the phase angle α with respect to the motion of the incident wave at the origin by

$$\alpha = \text{arc tan } (-\text{Im } p/\text{Re } p)$$

where Im means the imaginary part of what follows.

RESULTS AND DISCUSSIONS

The body plan of CGN-38 and the locations of the six pressure gages are shown in Figures 1 and 2, respectively. The principal particulars of the ship is given in Table 1.

The strip theory is based on the two-dimensional flow assumption at each transverse cross section of a body. Thus, the geometry of the immersed portion of a cross section is the basic information for pressure calculations. The shapes of the right-half cross section on the boundaries of which the pressure gages are mounted are shown in Figure 3. Approximately 10 to 13 line segments are used to represent the right half of the immersed contour in the computation.[5] The full-scale offsets of the points on the boundary of the cross sections used for the computation are shown in Table 2.

Comparison of the computed values of the pressure amplitudes with the measured results are shown in Figures 4 to 8. Since the presently used strip theory cannot be applied at the nose point of the dome, no computational results were obtained for the pressure gage 4; hence, no comparison is presented for this gage.

The vertical ordinate of the figures represent a nondimensionalized pressure amplitude defined by

$$\bar{P}_i = \frac{P_{io}}{\rho g \zeta_A (\nabla / L^3)} \tag{7}$$

where P_{io} = pressure amplitude at the ith gage

ρ = water density

g = gravitational acceleration

ζ_A = amplitude of incoming wave

∇ = displaced volume of ship

L = length between the perpendiculars

The computed pressure amplitudes are obtained by taking the absolute values of Equation (5) minus the static pressure ρgz and the pressure term associated with the surge motion, $i\rho\omega_E \xi_1 \phi_1$. The exclusion of the surge-related pressure is due to the assumption that the surge motion is small.

As can be readily observed in Equation (5), the pressure computation requires the information on ship motions, ξ_i. Unless the computation of the motions is reliable, the prediction of the pressure cannot be expected to be reliable. In Figure 9 comparison of the computed versus measured relative bow motion is presented. The relative bow motion is defined as the vertical motion of a point on the bow with respect to the collinear vertical motion of the free surface. The vertical motion of a point on the hull is given by Equation (6). As can be seen, three modes

of motion, heave, pitch and roll, constitute the vertical motion. The full-scale values of x and y of the measuring point are 83.56 m (Station 1/2) and -5.68 m (Starboard), respectively. The reason for showing the comparison of the relative motion instead of the individual modes of motion is that the vertical motion of the point on the hull is found to dominate the magnitude of the pressure amplitude at that point. Actually, the more relevant motion is the absolute motion; however, since the available measured motion is the relative bow motion, the comparison was made for the relative bow motion.

It is very intriguing to note the almost identical trends of the relative bow motion and the pressures. From Equation (5) one can readily observe that the major contribution to the oscillatory pressure should come from the change in the pressure head due to the vertical displacement of the point, i.e., $-\rho g\xi_v$. A closer examination indicates that the computed pressures can be decomposed in the following fashion

$$P_o = |P_w + P_s + P_v + P_h| \tag{8}$$

where P_w = pressure due to waves on restrained body

$$= -i\rho\omega(\phi_0+\phi_7) \tag{8a}$$

P_s = pressure equivalent to static head

$$= -\rho g\xi_v = -\rho g(\xi_3 - x\xi_5 + y\xi_4) \tag{8b}$$

P_v = pressure due to vertical acceleration and velocity of the body

$$= -i\rho\omega_E\phi_3\{\xi_3 - (x + \frac{12U}{\omega E})\xi_5\} \tag{8c}$$

P_h = pressure due to horizontal acceleration and velocity of the body

$$= -i\rho\omega_E\phi_2\{\xi_2 + (x + \frac{12U}{\omega_E})\xi_6\} \tag{8d}$$

As a typical illustration, the absolute magnitudes of P_o, P_w, P_s, P_v and P_h divided by $\rho g\zeta_A$* which are denoted by a bar sign, and the phase angles in degrees with respect to the motion of the incident wave at the origin are shown in Table 3 for P_3 for the bow-quartering waves. It is interesting to note that a major contribution to the total pressure comes from P_s and P_w. The contribution from the acceleration and velocity of the body seems almost negligible compared to that from

*The ratio $L^3/7$ is 416, hence these nondimensional pressures can be converted to the nondimensional values shown in Figure 7 by multiplying these values by 416.

the vertical displacement and wave motion. A close examination of P_w also reveals that for the waves longer than the ship length the major contribution comes from the incident wave, i.e.,

$$i\rho\omega\phi_0 = -\rho g\zeta_A e^{Kz - iK(x\cos\beta + y\sin\beta)}$$

or

$$|i\rho\omega\phi_0|/(\rho g\zeta_A) = e^{Kz} = e^{\frac{2\pi}{\lambda}z}$$

For $z = -6.9$ m at P_3 gage we get

$$|i\rho\omega\phi_0|/(\rho g\zeta_A) = e^{-43.35/\lambda}$$

where λ should be given in meters. It shows that for the wavelength greater than the ship length the contribution of the diffracted wave to $\overline{P}_w$ is less than 10 percent. As the wavelength becomes less than half of the ship length, contributions from the incident wave and the diffracted wave approach about the same.

If we ignore the contribution of $\overline{P}_v$ and $\overline{P}_h$ to $\overline{P}_o$, then we can approximate $\overline{P}_o$ by

$$\overline{P}_t = [\overline{P}_w^{\,2} + \overline{P}_s^{\,2} + 2\overline{P}_w\overline{P}_s\cos(\alpha_w - \alpha_s)]^{\frac{1}{2}} \qquad (9)$$

In Table 4 the values of $\overline{P}_t$ are shown together with $\overline{P}_o$ and the ratio of $\overline{P}_t/\overline{P}_o$ in percent. One can readily observe that the errors caused by the approximation is within 15 percent. For $\lambda > L$, the error is reduced to less than 10 percent. Although the results are not presented for the other pressures, it was found that the same trend is applicable to the others. In Table 5 comparison of the relative magnitudes of the pressure components for P_2 and P_5 is shown for $U = 20$ knots. It is interesting to note that for the gage P_2 which is located at the side of the sonar dome we find $\overline{P}_h > \overline{P}_v$, and for P_5 which is located on the bottom we find $\overline{P}_v > \overline{P}_h$. This fact implies that the mode of motion which is in the direction normal to the point on the body surface contributes significantly larger pressure than the mode in tangent to the point. However, $\overline{P}_v$ and $\overline{P}_h$ are still much smaller magnitudes compared to $\overline{P}_s$ and $\overline{P}_w$.

It should be noted that P_s, which is only dependent upon the absolute vertical motion (see Equation (8b)), should not vary over the sonar surface very much since the variation in x and y over the surface has a negligibly small effect on the

vertical motion. Thus, it is expected that the difference in $\overline{P}_o$ among the different gages is attributed mainly to $\overline{P}_w$.

The comparisons shown in Figures 4 through 8 show that except for P_3 and P_6 the computed pressure amplitudes tend to overpredict for wavelengths greater than those at which the peak amplitudes are obtained. A close examination of the comparison of the relative bow motion in Figure 9 shows a similar trend. Thus, it can be concluded that for longer waves, the accuracy of the pressure prediction at a point depends directly upon the accuracy of the prediction of the absolute vertical motion of the point.

A large discrepancy can be observed between the computed and measured pressures at P_5 for shorter waves and greater speeds. This is the point located at the bottom side of the sonar dome, see Figure 2. It appears that the discrepancy does not originate from the vertical motion since the agreement between the computed and the measured values is very good for the entire range of wavelength and the forward speed, see Figure 9. Thus, it implies that the contribution from sources other than the vertical motion should be the cause of the discrepancy. Here, the evidence of the failure of the strip theory is clearly demonstrated. It is unclear why the effect of the fluid disturbances associated with the velocity potentials ϕ_j becomes more significant at this location. At the full-scale speed of 10 knots, agreement is good for both head and oblique waves, see Figure 7. However, at the higher speeds the measured peak value of P_5 is about 18 percent greater than that of P_3 at 30 knots in head waves, whereas the computed peak value of P_5 is about 22 percent less than that of P_3. A further investigation is needed to find out a rational explanation of the discrepancy at P_5.

The comparisons made in this report are limited to the first-order oscillatory pressure amplitudes. As described in Reference 1, the total pressures measured from the pressure gages exhibited steady pressures (mean shifts), the values of which were different from those measured in calm water. This fact demonstrates the evidence that the second-order steady pressures resulting from the oscillatory fluid disturbances should be taken into account if an accurate total pressure (steady plus the oscillatory) at a point on the hull is to be computed. An attempt was made to compute the second-order steady pressure by $\frac{\rho}{4}\dot{\xi}_R\dot{\xi}_R^*$ where $\xi_R = \dot{\xi}_3 - x\dot{\xi}_5 + y\dot{\xi}_4 + U\xi_5 - \omega A\, e^{Kz - iK(x\cos\beta + y\sin\beta)}$ and ξ_R^* is the conjugate of ξ_R. The values, however, turned out to be negligibly small.

SUMMARY

The first-order pressures obtained by Equation (5) using the strip theory were compared with the measured pressures at five locations in the sonar dome of a CGN-38 model proceeding in waves.

In general, a good agreement between the two results were obtained except for the pressures at high speed at the bottom side of the dome (referred to in the text as P_5). It was found that the good agreement was due to the fact that the major contribution to the pressure results from the pressure head change due to the vertical displacement of the point during the wave excited motion, and that the strip theory predicts this vertical displacement reasonably well. The second major contribution to the pressures is found to be associated with the wave motion, and the last and the smallest contribution comes from the oscillatory motion of the body. This statement may not be applicable to the pressures on the bottom side of the dome as evidenced by the discrepancy found for P_5. A search for a rational explanation for the failure of the strip theory for the pressures on the bottom side of the dome is left for a future investigation.

ACKNOWLEDGMENTS

The authors would like to extend their gratitude to Mr. V.J. Monacella who has induced the authors to participate in the project and offered technical consultations when needed. The authors also would like to acknowledge the close cooperation provided by Lewis E. Motter who conducted the model experiment.

REFERENCES

1. Motter, L.E., "Hydrodynamic Pressure Measurement on the Sonar Dome of a CGN-38 Class Model," Report DTNSRDC/SPD-0991-01, in preparation.

2. Salvesen, N. et al., "Ship Motion and Sea Loads," Trans. Society of Naval Architects and Marine Engineers, Vol. 18 (1970).

3. Meyers, W.G. et al., "User's Manual for the Standard Ship Motion Program, SMP," Report DTNSRDC/SPD-0946-01, in preparation.

4. Newman, J.N., "Marine Hydrodynamics," the MIT Press, Cambridge, Mass. (1977).

5. Frank, W., "Oscillation of Cylinders in or below the Free Surface of Deep Fluids," Naval Ship Research and Development Center Report 2375 (1967).

6. Pien, P.C. and C.M. Lee, "Motion and Resistance of a Low-Waterplane Catamaran," The 9th Naval Hydrodynamic Symposium, Paris; Proceedings published by the Office of Naval Research (1972).

TABLE 1 - CGN-38 CLASS SHIP PARTICULARS

Parameter	Value	
	Ship	Model
Displacement	12,223 M. Ton S.W. (12,031 L. Tons S.W.)	855.31 kg (1885.6 lbs F.W.)
Length between Perpendiculars	170.69 m (560.0 ft)	7.09 m (23.27 ft)
Draft	6.92 m (22.7 ft)	0.29 m (0.94 ft)
Beam at Midship	18.87 m (61.9 ft)	0.78 m (2.57 ft)
Longitudinal Center of Gravity. LCG, aft of Midship	2.49 m (8.16 ft)	0.10 m (0.34 ft)
Vertical Center of Gravity, KG (Relative to Waterline)	0.71 m (2.32 ft)	0.03 m (0.10 ft)
Transverse Metacentric Height, GM	1.48 m (4.84 ft)	0.06 m (0.20 ft)
Scale Ratio	24.064	

TABLE 2 - OFFSETS OF CROSS SECTIONS CONTAINING PRESSURE GAGES (IN METERS)

P_1 and P_6 (5.90)*		P_2 (4.75)		P_3 (3.78)		P_5 (4.17)	
y	z	y	z	y	z	y	z
0.	-9.244						
1.222	-9.121	0.	-9.036	0.	-8.307	0.	-8.808
2.188	-8.803	1.222	-8.840	0.740	-8.209	0.465	-8.796
2.714	-8.376	1.993	-8.425	1.229	-7.756	1.033	-8.557
2.983	-7.777	2.445	-7.777	1.229	-7.256	1.601	-8.245
2.995	-7.165	2.445	-7.165	0.947	-6.889	1.938	-7.726
2.702	-6.554	2.078	-6.554	0.202	-6.552	1.840	-7.139
1.834	-6.591	0.550	-5.637	0.061	-5.953	1.235	-6.497
0.966	-5.637	0.324	-5.026	0.147	-5.036	0.617	-6.124
0.562	-5.026	0.306	-4.109	0.232	-3.533	0.293	-5.691
0.489	-4.109	0.428	-2.581	0.318	-2.237	0.220	-4.731
0.587	-2.581	0.575	-1.359	0.477	-1.119	0.282	-3.539
0.746	-1.359	0.770	0.	0.617	0.	0.483	-1.381
0.954	0.					0.697	0.

*Longitudinal location from FP.

TABLE 3 - COMPARISON OF COMPUTED PRESSURE COMPONENTS OF P_3 FOR BOW-QUARTERING WAVES

Speed (knot)	λ/L	Pressure Amplitude/($\rho g \zeta_A$)					Phase Angles (degrees)				
		$\bar{P}_o$	$\bar{P}_w$	$\bar{P}_s$	$\bar{P}_v$	$\bar{P}_h$	α_o	α_w	α_s	α_v	α_h
0	1.45	1.17	0.88	1.62	0.04	0.14	-160	94	-126	-61	152
	1.00	1.93	0.85	1.86	0.07	0.15	-149	135	-121	-66	152
	0.50	1.75	0.83	0.85	0.06	0.09	-108	-94	-118	-83	-161
	0.30	1.06	0.73	0.58	0.06	0.07	30	71	-17	4	9
10	1.95	0.86	0.90	1.54	0.04	0.10	-165	69	-135	-65	141
	1.41	1.48	0.87	1.89	0.07	0.13	-159	96	-131	-72	136
	1.08	2.28	0.85	2.22	0.11	0.16	-154	125	-131	-81	144
	0.51	1.71	0.83	1.11	0.11	0.09	-148	-100	-177	-153	177
	0.31	0.71	0.75	0.19	0.03	0.04	32	51	-66	-54	-10
20	2.05	0.92	0.90	1.63	0.05	0.09	-166	66	-139	-71	128
	1.57	1.54	0.88	2.00	0.08	0.12	-162	86	-137	-79	129
	1.03	3.28	0.85	2.84	0.19	0.18	-164	131	-149	-108	131
	0.55	1.02	0.83	0.71	0.09	0.08	-171	-116	133	153	164
	0.34	0.89	0.78	0.10	0.02	0.03	16	-87	-78	-24	6
30	2.13	1.01	0.91	1.72	0.06	0.09	-168	63	-142	-77	121
	1.53	2.00	0.88	2.32	0.12	0.14	-167	89	-145	-94	120
	1.00	4.35	0.84	3.44	0.29	0.17	175	135	-177	-144	115
	0.50	0.71	0.83	0.19	0.04	0.04	-110	-95	125	139	-162

TABLE 4 - APPROXIMATION OF P_o BY P_w AND P_s FOR P_3 FOR BOW-QUARTERING WAVES BY EQUATION (9)

Speed (knot)	λ/L	$\lvert P_t \rvert/(\rho g \zeta_A)$	$\lvert P_o \rvert/(\rho g \zeta_A)$	$(\lvert P_t \rvert/\lvert P_o \rvert) \times 100$
0	1.45	1.10	1.17	94
	1.00	1.85	1.93	96
	0.50	1.64	1.75	94
	0.30	0.90	1.06	85
10	1.95	0.81	0.86	94
	1.41	1.44	1.48	97
	1.08	2.17	2.28	95
	0.51	1.53	1.71	89
	0.31	0.68	0.71	96
20	2.05	0.90	0.92	98
	1.57	1.48	1.54	96
	1.03	3.10	3.28	95
	0.55	0.88	1.02	86
	0.34	0.88	0.89	99
30	2.13	0.97	1.01	96
	1.53	1.94	2.00	97
	1.00	4.05	4.36	93
	0.50	0.69	0.71	98

TABLE 5 - COMPARISON OF COMPUTED PRESSURE COMPONENTS OF P_2 AND P_5 FOR BOW-QUARTERING WAVES AT U = 20 KNOTS

	P_2				P_5			
λ/L	2.40	1.57	1.14	0.3	2.05	1.57	1.03	0.39
$\bar{P}_o$	0.58	1.53	2.68	0.66	0.81	1.31	2.55	0.38
$\bar{P}_w$	0.89	0.86	0.83	0.64	0.82	0.78	0.68	0.38
$\bar{P}_s$	1.42	2.06	2.67	0.06	1.63	2.00	2.83	0.07
$\bar{P}_v$	0.03	0.04	0.03	0.01	0.10	0.16	0.40	0.04
$\bar{P}_h$	0.09	0.17	0.23	0.04	0.01	0.01	0.02	0.00

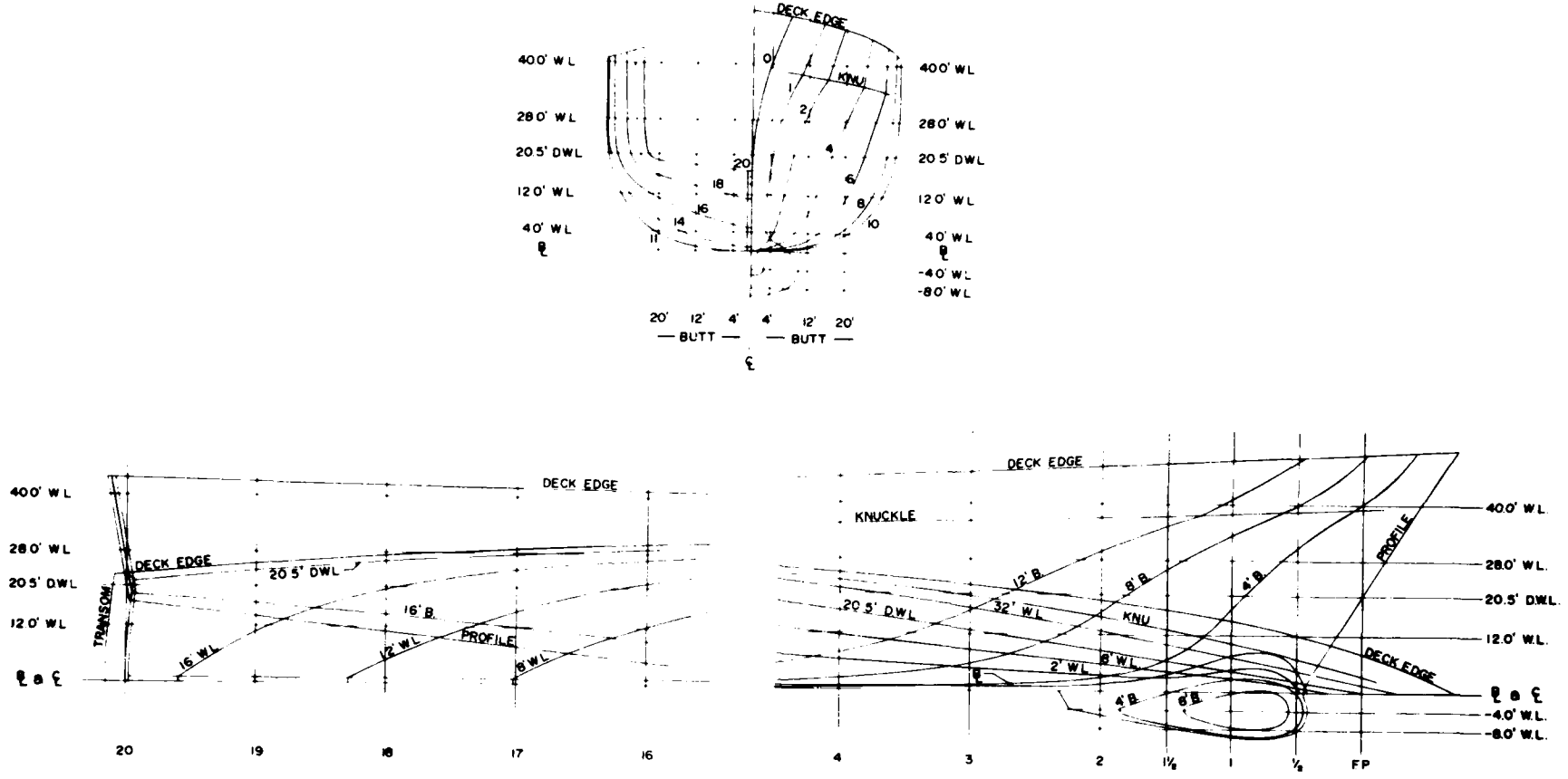

Figure 1 - Body Plan, Waterplane, and Profile of CGN 38

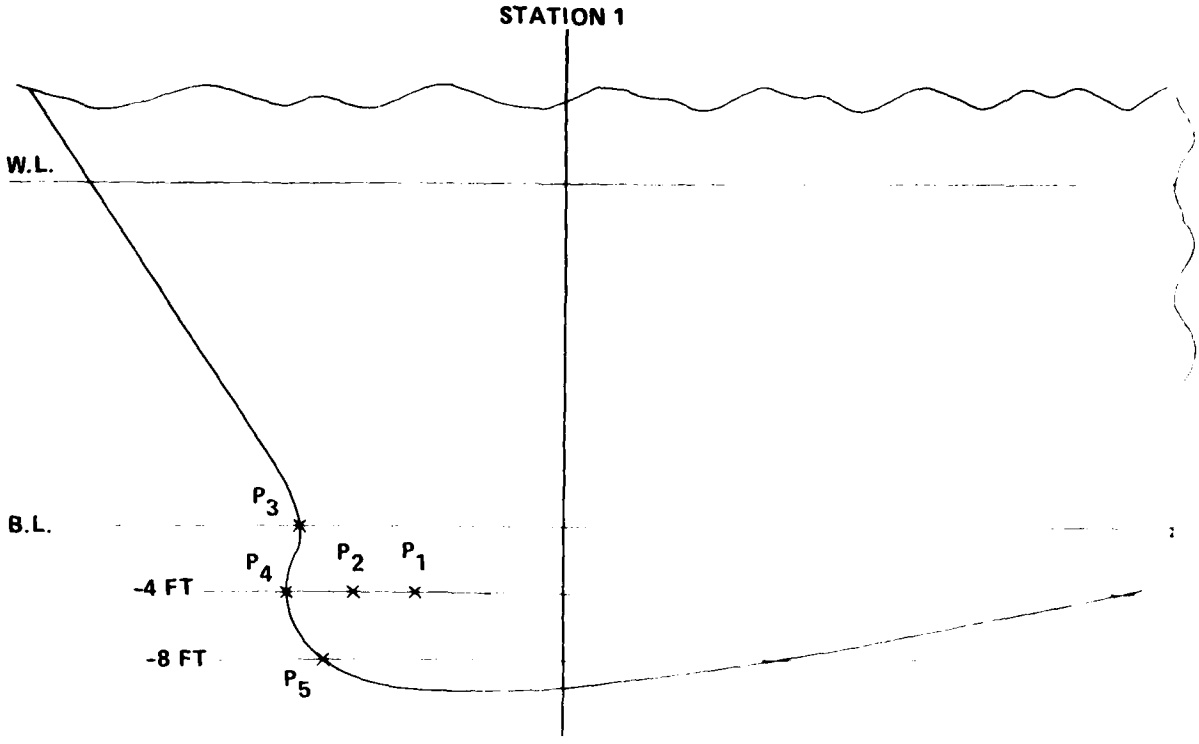

CENTERLINE PROFILE VIEW

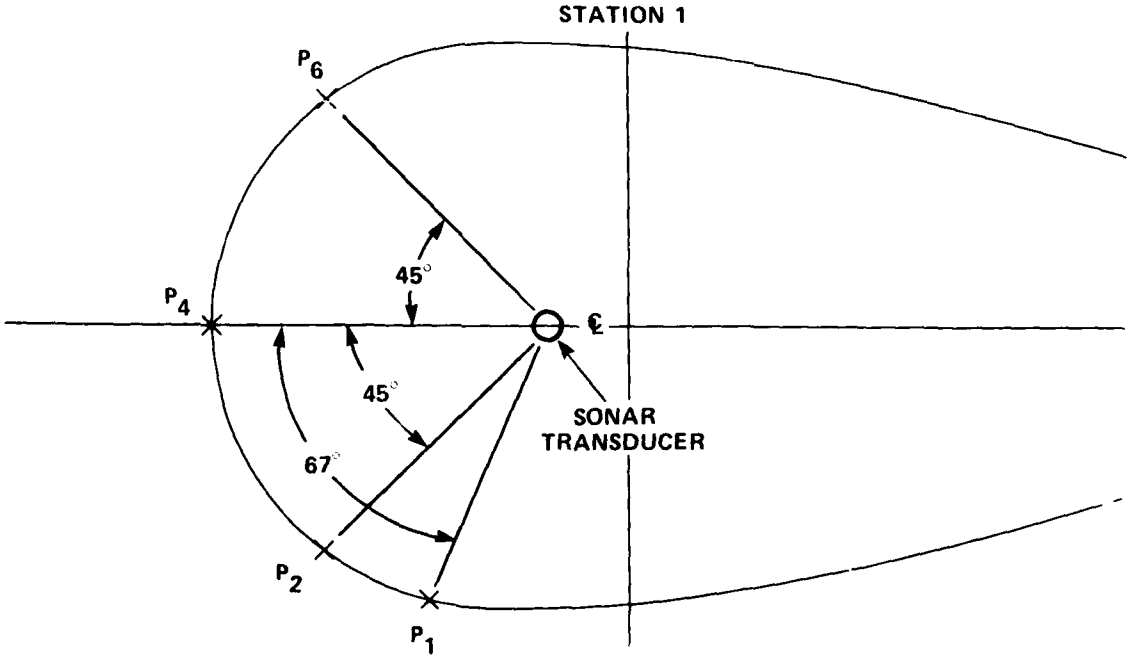

SONAR DOME CROSS SECTION AT
-4 FT WATERLINE

Figure 2 - Pressure Gage Locations

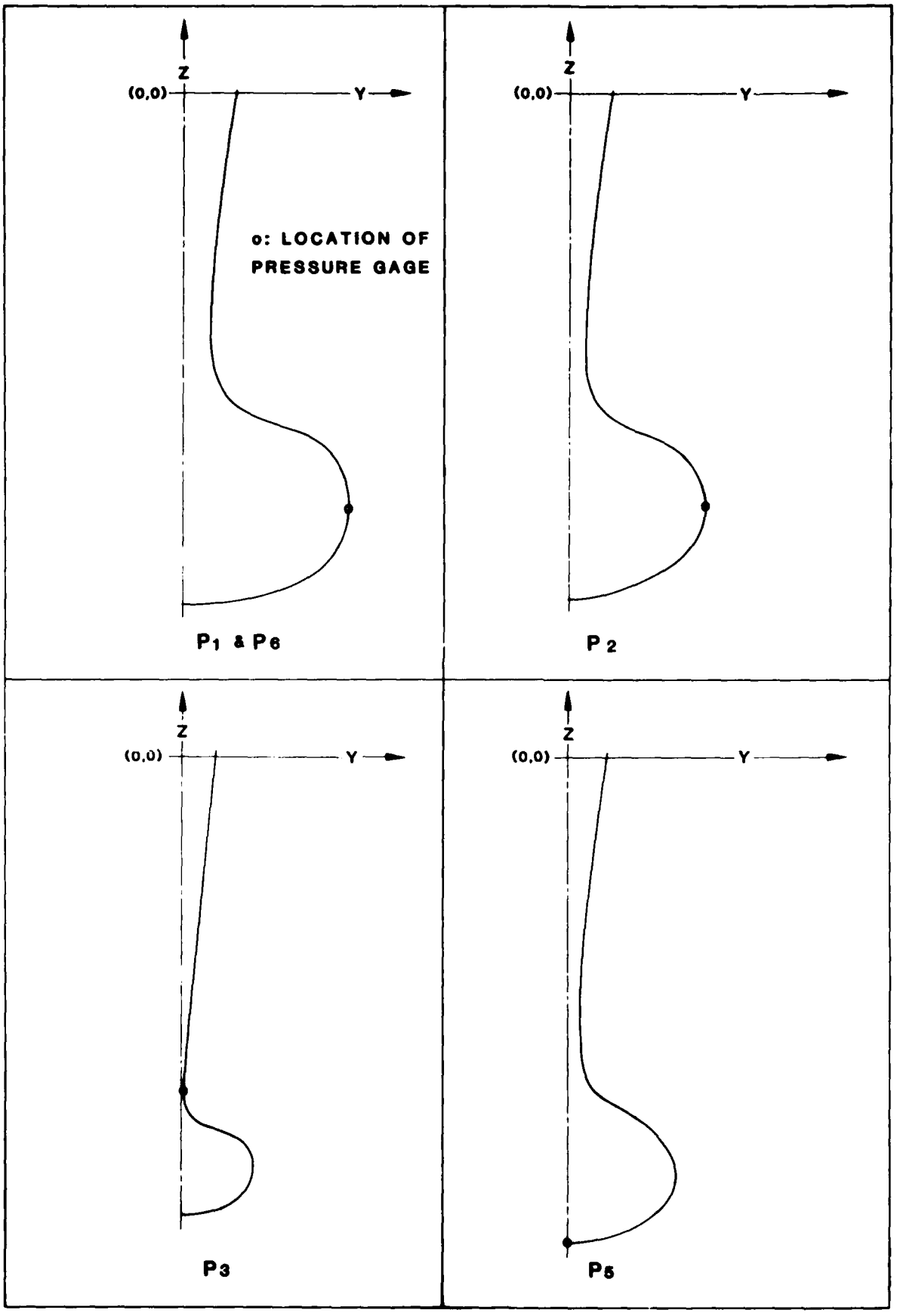

Figure 3 - Cross Sections Containing
Pressure Gage(s)

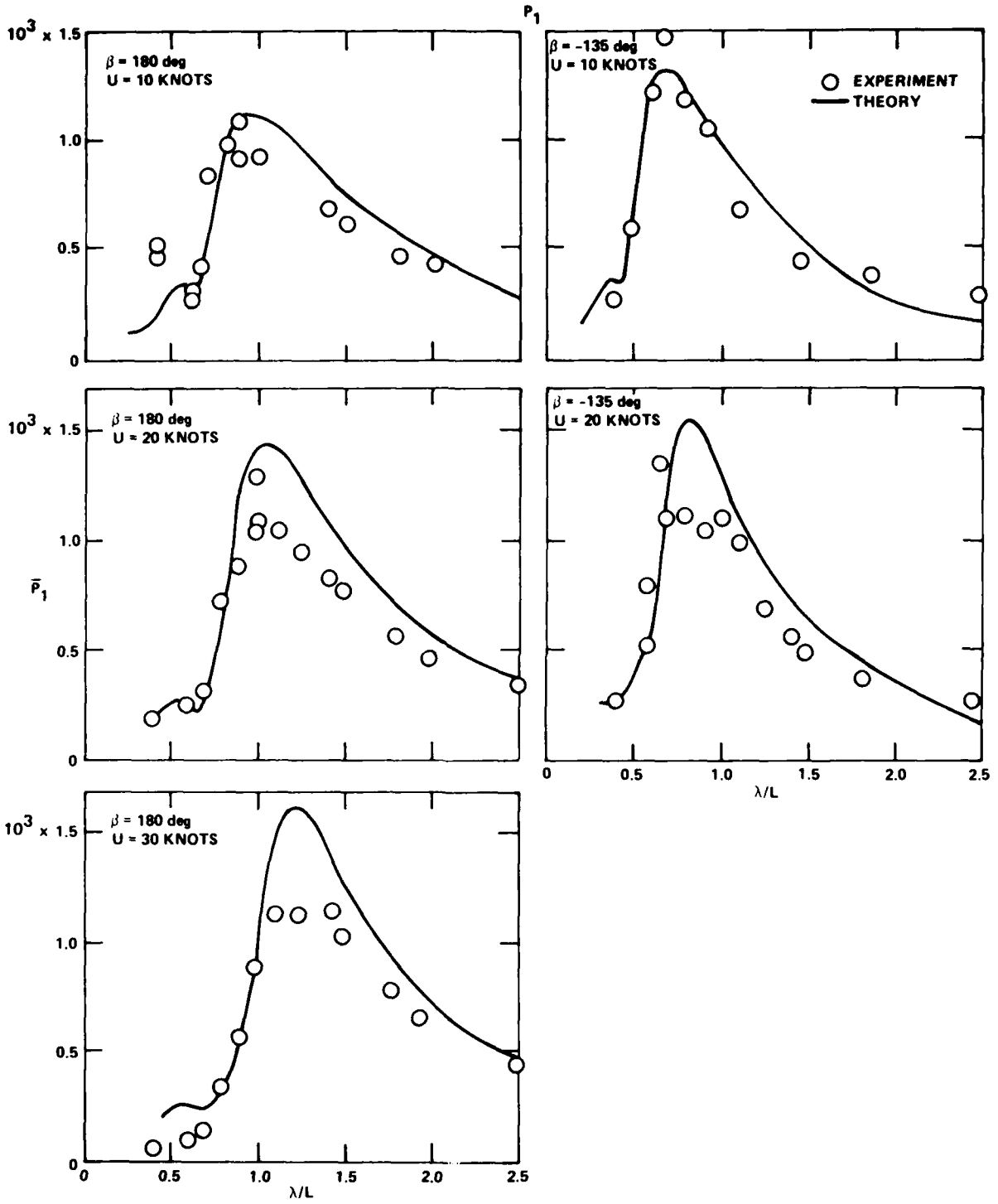

Figure 4 - Pressure Amplitude of P_1 versus Wave Length

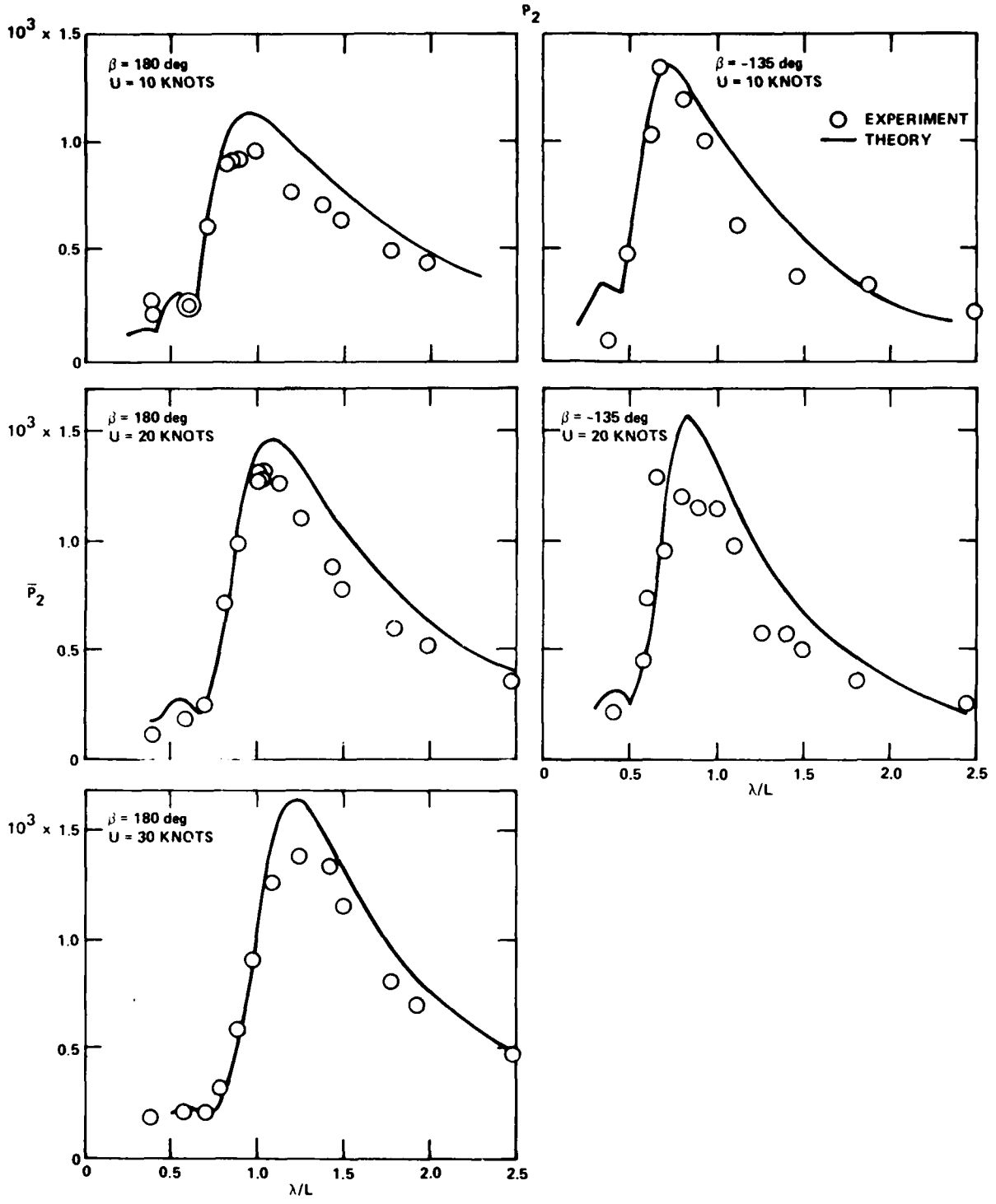

Figure 5 - Pressure Amplitude of P_2 versus Wave Length

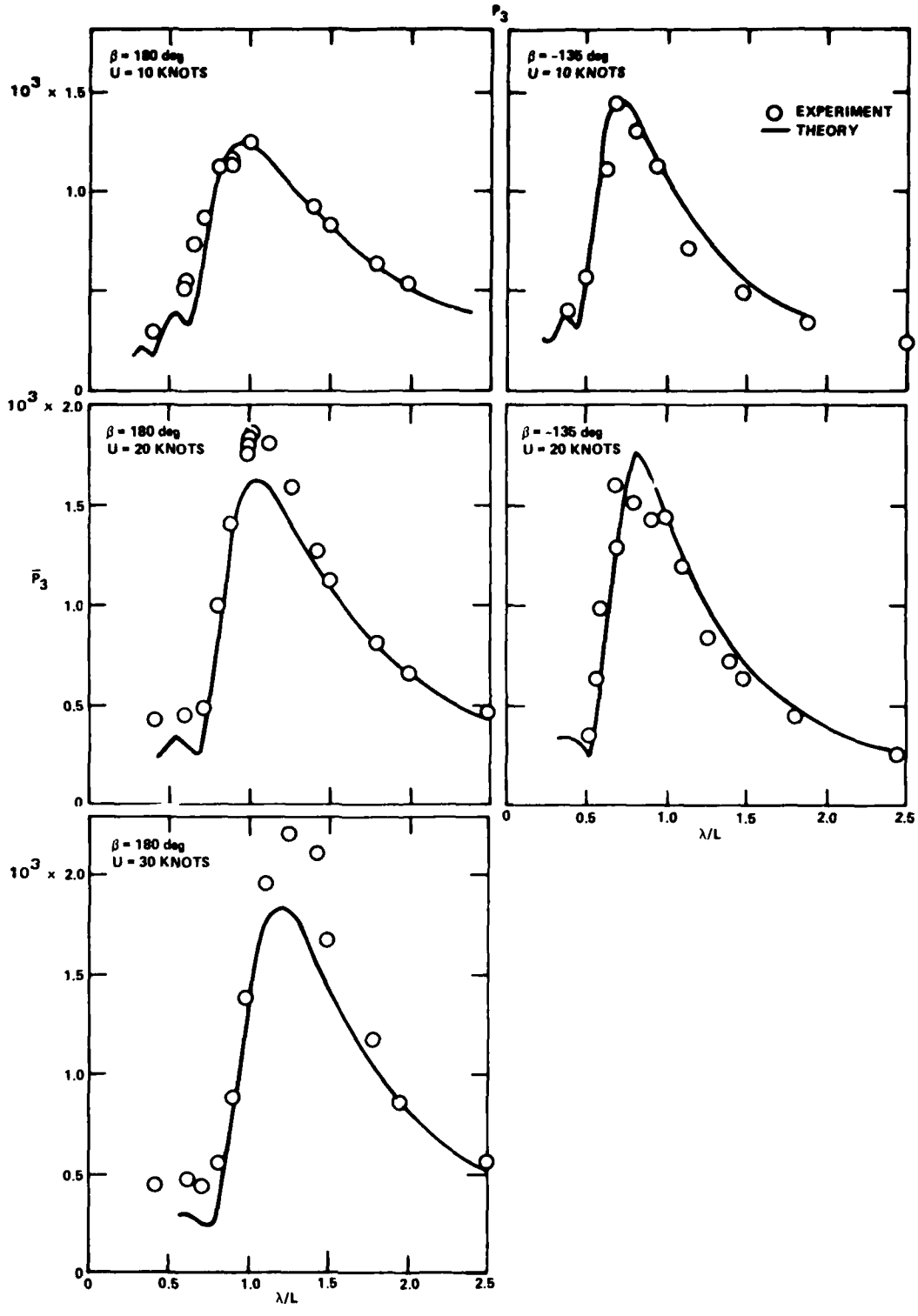

Figure 6 - Pressure Amplitude of P_3 versus Wave Length

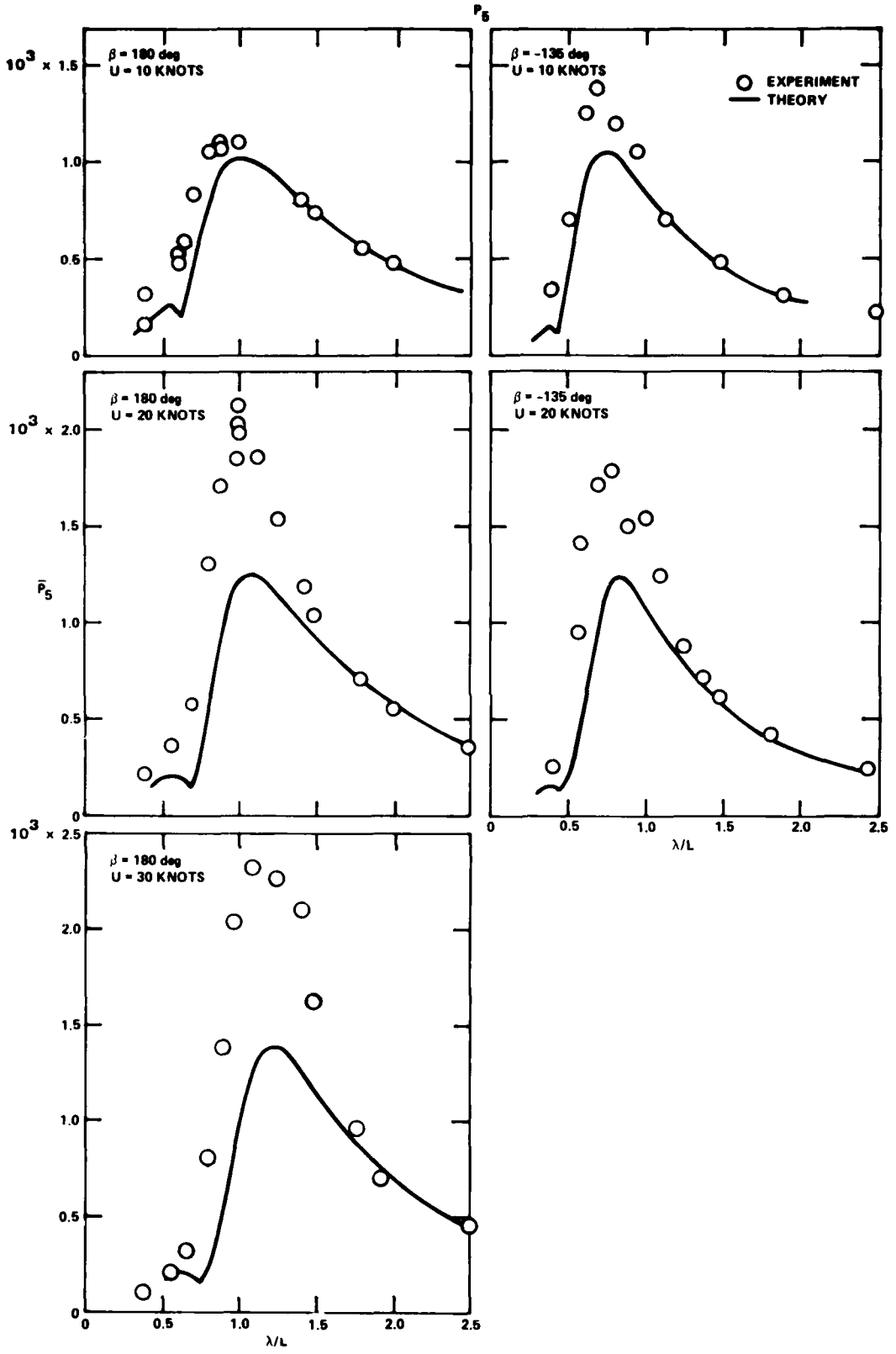

Figure 7 - Pressure Amplitude of P_5 versus Wave Length

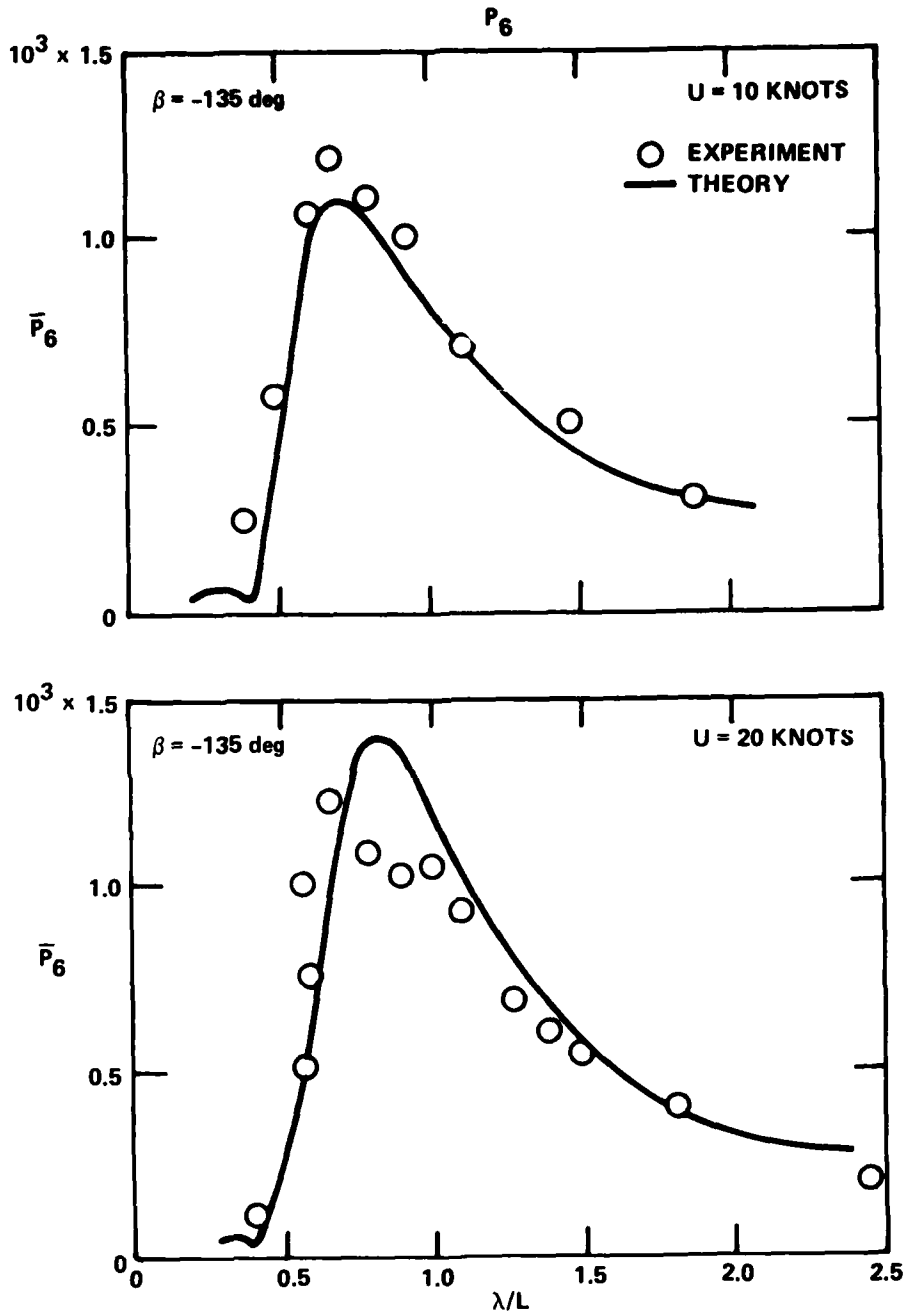

Figure 8 - Pressure Amplitude of P_6 versus Wave Length

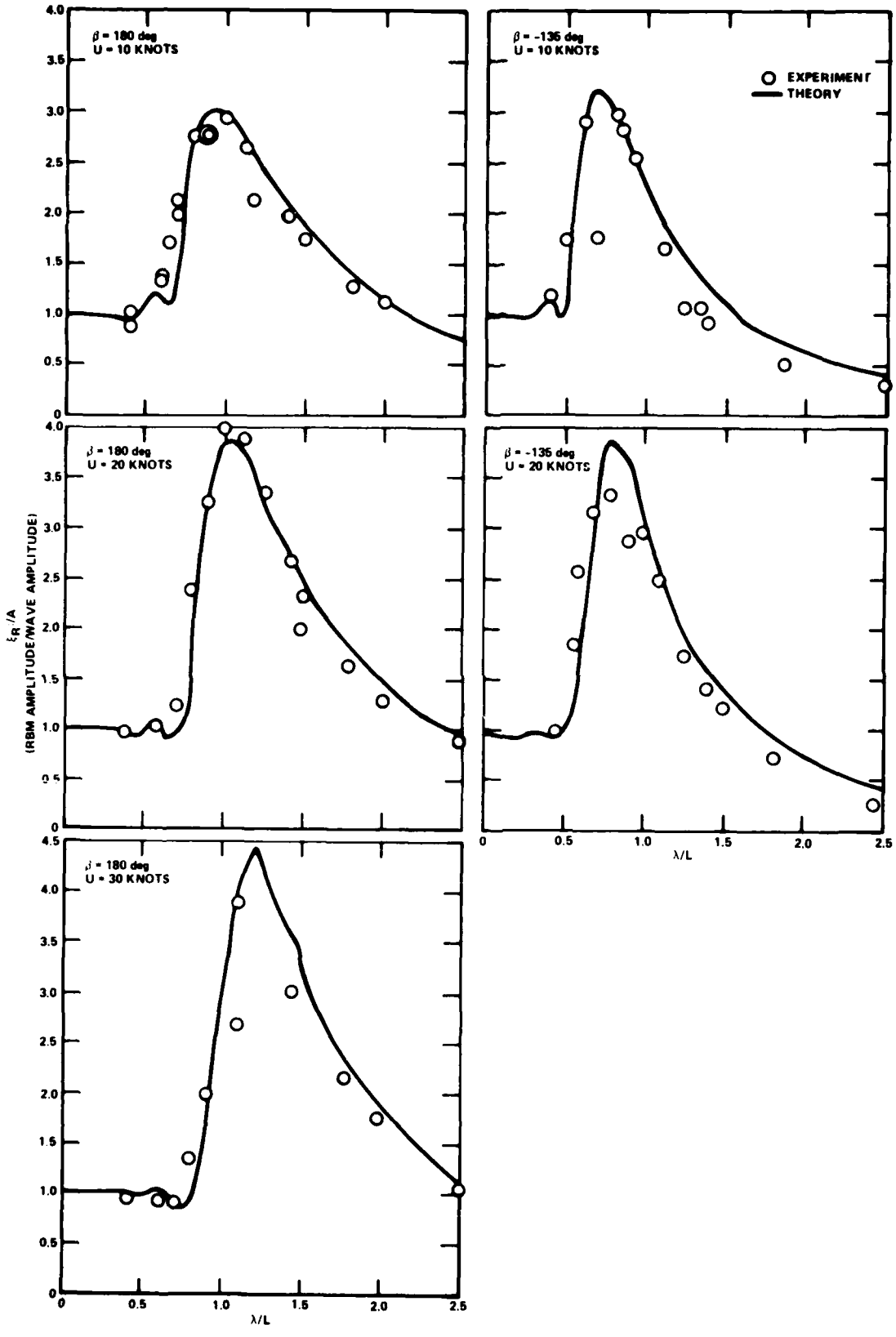

Figure 9 - Relative Bow Motion in Regular Waves at x = 83.56m (Station ½) and y = -5.68m

DTNSRDC ISSUES THREE TYPES OF REPORTS

1. DTNSRDC REPORTS, A FORMAL SERIES, CONTAIN INFORMATION OF PERMANENT TECHNICAL VALUE. THEY CARRY A CONSECUTIVE NUMERICAL IDENTIFICATION REGARDLESS OF THEIR CLASSIFICATION OR THE ORIGINATING DEPARTMENT.

2. DEPARTMENTAL REPORTS, A SEMIFORMAL SERIES, CONTAIN INFORMATION OF A PRELIMINARY, TEMPORARY, OR PROPRIETARY NATURE OR OF LIMITED INTEREST OR SIGNIFICANCE. THEY CARRY A DEPARTMENTAL ALPHANUMERICAL IDENTIFICATION.

3. TECHNICAL MEMORANDA, AN INFORMAL SERIES, CONTAIN TECHNICAL DOCUMENTATION OF LIMITED USE AND INTEREST. THEY ARE PRIMARILY WORKING PAPERS INTENDED FOR INTERNAL USE. THEY CARRY AN IDENTIFYING NUMBER WHICH INDICATES THEIR TYPE AND THE NUMERICAL CODE OF THE ORIGINATING DEPARTMENT. ANY DISTRIBUTION OUTSIDE DTNSRDC MUST BE APPROVED BY THE HEAD OF THE ORIGINATING DEPARTMENT ON A CASE-BY-CASE BASIS.